EUKARYOTIC CELL, July 2009, p. 977–989 Vol. 8, No. 7
1535-9778/09/$08.00+0 doi:10.1128/EC.00009-09

Ustilago maydis Rho1 and 14-3-3 Homologues Participate in Pathways Controlling Cell Separation and Cell Polarity▽†

Cau D. Pham,[1] Zhanyang Yu,[1]‡ Björn Sandrock,[2] Michael Bölker,[2] Scott E. Gold,[3] and Michael H. Perlin[1]*

Department of Biology, Program on Disease Evolution, University of Louisville, Louisville, Kentucky[1]; Department of Biology, Philipps-Universität, Marburg, Germany[2]; and Department of Plant Pathology, University of Georgia, Athens, Georgia[3]

Received 6 January 2009/Accepted 23 April 2009

Proteins of the 14-3-3 and Rho-GTPase families are functionally conserved eukaryotic proteins that participate in many important cellular processes such as signal transduction, cell cycle regulation, malignant transformation, stress response, and apoptosis. However, the exact role(s) of these proteins in these processes is not entirely understood. Using the fungal maize pathogen, *Ustilago maydis*, we were able to demonstrate a functional connection between Pdc1 and Rho1, the *U. maydis* homologues of 14-3-3ε and Rho1, respectively. Our experiments suggest that Pdc1 regulates viability, cytokinesis, chromosome condensation, and vacuole formation. Similarly, *U. maydis* Rho1 is also involved in these three essential processes and exerts an additional function during mating and filamentation. Intriguingly, yeast two-hybrid and epistasis experiments suggest that both Pdc1 and Rho1 could be constituents of the same regulatory cascade(s) controlling cell growth and filamentation in *U. maydis*. Overexpression of *rho1* ameliorated the defects of cells depleted for Pdc1. Furthermore, we found that another small G protein, Rac1, was a suppressor of lethality for both Pdc1 and Rho1. In addition, deletion of *cla4*, encoding a Rac1 effector kinase, could also rescue cells with Pdc1 depleted. Inferring from these data, we propose a model for Rho1 and Pdc1 functions in *U. maydis*.

Morphological switching is a unique attribute of all dimorphic fungi, which alternate between budding and filamentous growth. In some cases, as with mating, this is a prerequisite for genetic diversity for this subfamily of fungi. In addition, many dimorphic fungal pathogens rely on this ability in order to effectively invade their host. In general, the transition between these alternate life forms means a complete turnover of cellular and proteomic components, which often involves cell cycle arrest and/or cytoskeletal rearrangement. Although the cellular proteomes associated with these two processes share many components, there are both temporal and spatial regulations that are manifested during the transitional phase (4).

Temporal-spatial regulation of the proteome during the dimorphic transition requires cooperation and synchronized communication among different regulatory pathways. Two highly intricate, yet well-established, signaling cascades that regulate fungal morphogenesis are the mitogen-activated protein kinase (MAPK) (34, 46) and protein kinase A pathways (11). These signaling cascades detect and perpetuate extracellular stimuli, e.g., pheromones and nutrients, which lead to phase transitions in dimorphic fungi. Although the mechanisms are not as fully understood, members of two highly conserved families of proteins, Rho/Rac GTPases and 14-3-3 proteins, have also been shown to control filamentation. Constituents of the Rho/Rac protein family have been shown to regulate actin organization (26, 35, 36), cytokinesis (3, 49, 52), cell integrity (42, 56), pathogenicity (29), signal transduction (22, 44, 56), and cell migration (8). Their activity is dependent upon the reversible binding of guanine nucleotides catalyzed by guanine nucleotide exchange factors (GEFs) and GTPase activating proteins (GAPs) (15, 22, 23, 25, 44). Upon activation, Rho-GTPases stimulate downstream effector proteins such as p21-activated kinases (PAKs) (29, 51) or Rho kinase (ROCK) (36). Based on in silico analysis of the genome sequence, the fungal pathogen of maize, *Ustilago maydis*, contains six different Rho/Rac encoding genes: *cdc42*, *rac1*, and four additional genes predicted to encode Rho-like proteins (20). Of these, only the roles of Cdc42 and Rac1 have been examined in depth. Cdc42 was shown to regulate cytokinesis, while Rac1 regulates hyphal development in *U. maydis* (26). We examine here the place of a Rho1 homologue, Rho1, in *U. maydis* cell morphology, polarity, and development.

Similarly, the highly conserved, ubiquitously expressed 14-3-3 proteins that are found in most eukaryotes have also been shown to contribute to cellular differentiation and cytoskeletal organization. Like Rho-GTPases, 14-3-3 proteins play multiple roles, in cytoskeletal function, cell cycle regulation, apoptosis, and the regulation of a variety of signaling pathways (17, 19, 33, 50). These acidic proteins have been found in each cellular compartment and most organisms examined possess multiple isoforms: seven isoforms are found in mammals, and as many as fifteen isoforms have been identified in plants (31). Interestingly, the yeast *Saccharomyces cerevisiae*, the fruit fly, *Drosophila melanogaster*, and the nematode, *Caenorhabditis elegans*, each possess only two 14-3-3 isoforms (50), while *Candida albicans* contains a single isoform (37). They function

* Corresponding author. Mailing address: Department of Biology, Program on Disease Evolution, University of Louisville, Louisville, KY 40292. Phone: (502) 852-5944. Fax: (502) 852-0725. E-mail: mhperl01@gwise.louisville.edu.

† Supplemental material for this article may be found at http://ec.asm.org/.

‡ Present address: Neuroprotection Research Laboratory, Departments of Neurology and Radiology, Massachusetts General Hospital, and Program in Neuroscience, Harvard Medical School, Boston, Massachusetts.

▽ Published ahead of print on 1 May 2009.

typically by binding their particular ligands at phosphoserine or phosphothreonine residues (50). It is not clear what 14-3-3 proteins do in the processes mentioned above, whether they act as scaffolds or effectors. Inspection of the *U. maydis* genome sequence revealed that this organism could be ideal for the study of 14-3-3 proteins because, unlike most other organisms, the *U. maydis* genome contains only a single 14-3-3 homologue. Due to its predicted binding of phosphorylated proteins, we named this homologue Pdc1 (for phosphorylation domain coupling protein [10]). Recently, the protein (also designated Bmh1 [32]) was also shown to be involved in cell cycle regulation.

Despite the functional differences between Rho-GTPases and 14-3-3 proteins, we provide evidence that members of these two families participate in the same regulatory cascade(s) that control morphogenesis in the dimorphic fungus *U. maydis.* We are able to demonstrate that both Pdc1 and Rho1 are essential for cell viability. In addition, overexpression of Rho1 led to the reduction of filamentation. Overexpression of Rac1 triggers filamentation in *U. maydis* (13, 29). We show here that deleting Rac1 eliminates the lethal effect imposed by either Rho1 or Pdc1 depletion. Our results have led us to predict that both Rho1 and Pdc1 are negative regulators of Rac1 in *U. maydis* and that they play important roles in polarized growth and cytokinesis.

MATERIALS AND METHODS

Strains and growth conditions. *U. maydis* strains utilized in the present study are listed in Table 1. *Escherichia coli* strains, DH5α (Bethesda Research Laboratories) and TOP10 (Invitrogen), were used for all cloning and plasmid amplification requirements. The yeast strains L6247 (*ura3-52 leu2*::*hisG his3*::*hisG bmh2*::*HIS3*$^+$ *bmh1*::*HIS3*$^+$; a gift of G. Fink, Massachusetts Institute of Technology) and Y187 and AH109 (Clontech) were used for complementation and yeast two-hybrid experiments, respectively.

U. maydis cells were grown at 28°C in YEPS, YEPS-light, and PDA as described previously (6). Induction or suppression of the P_{crg1} promoter was carried out by growing cells in either YP (1% yeast extract and 2% peptone) or minimal medium (0.17% yeast nitrogen base [YNB] and 0.2% ammonium sulfate) supplemented with 2% arabinose or 2% dextrose, respectively (5). Similarly, induction or suppression of P_{nar1} promoter was achieved by growing cells in minimal media (0.17% yeast nitrogen base and 2% glucose) supplemented with 0.2% potassium nitrate ($MMNO_3$ medium) or 0.2% ammonium sulfate, respectively (4, 5). Mating medium and solid medium were made with 1% activated charcoal and/or 2% agar (14).

For yeast complementation and yeast two-hybrid experiments, cells were grown on SD medium (0.17% YNB and 1× amino acid dropout solution) supplemented with dextrose or galactose. For complementation assays, yeast cells were plated onto SD medium containing either glucose (repressor of yeast P_{GAL1} promoter) or galactose (inducer of P_{GAL1} promoter) and were kept at 25°C or 37°C for 3 days.

Yeast two-hybrid analyses. Yeast two-hybrid was performed according to the BD Matchmaker library construction and screening kit user manual (BD Biosciences, Palo Alto, CA), with modifications as indicated here. The pGBKT7 contains unique restriction sites in frame with the 3′ end of the GAL4 DNA-binding domain (BD) for constructing fusion proteins with a bait protein. For each known target protein the respective gene was cloned into this vector and used in conjunction with the prey vector, pGADT7, for two-hybrid analyses. pGADT7 is the DNA activation domain (AD) vector included with Matchmaker Two-Hybrid System 3, with unique restriction sites in frame with the 3′ end of the GAL4 AD for constructing a fusion protein with either a protein of interest or a fusion protein library.

Yeast haploid strains AH109 (*MAT***a** *trp1-901 leu2-3,112 ura3-52 his3-200 gal4*Δ *gal80*Δ *LYS2*::$GAL1_{UAS}$-$GAL1_{TATA}$-*HIS3* $GAL2_{UAS}$-$GAL2_{TATA}$-*ADE2 URA3*::$MEL1_{UAS}$-$MEL1_{TATA}$-*lacZ*) and Y187 (genotype: *MAT*α *ura3-52 his3-200 ade2-101 trp1-901 leu2-3,112 gal4*Δ *met*$^{--}$ *gal80*Δ *URA3*::$GAL1_{UAS}$-$GAL1_{TATA}$-*lacZ*) were also obtained from the kit and, separately, from the laboratory of S. Ellis (University of Louisville).

TABLE 1. Strains and plasmids

Strain or plasmid	Genotype	Source or reference
Strains		
1/2	*a1b1*	11
rho1^{crg1}	*a1b1 rho1*::P_{crg1}-*rho1*-*hyg*^{R}	This study
pdc1^{nar1}	*a1b1 pdc1*::P_{nar1}-*pdc1*-*cbx*^{R}	This study
pdc1^{crg1}	*a1b1 pdc1*::P_{crg1}-*pdc1*-*hyg*^{R}	This study
rho1^{crg1}*pdc1*^{nar1}	*a1b1 rho1*::P_{crg1}-*rho1*-*hyg*^{R}, *pdc1*::P_{nar1}-*pdc1*-*cbx*^{R}	This study
1/2pUM-Rho1	*a1b1*/pUM-*rho1*	This study
2/9	*a2b2*	11
2/9pUM-Rho1	*a2b2*/pUM-*rho1*	This study
BUB8	*a2b4*	26, 41
Bub8*rho1*^{crg1}	*a2b4 rho1*::P_{crg1}-*rho1*-*cbx*^{R}	This study
Bub8*pdc1*^{crg1}	*a2b4 rho1*::P_{crg1}-*pdc1*-*cbx*^{R}	This study
Bub8Δ*rac1*	*a2b4 rac1*::*nour*^{R}	29
Δ*rac1 rho1*^{crg1}	*a2b4 rac1*::*nour*^{R} *rho1*::P_{crg1}-*rho1*-*cbx*^{R}	This study
Δ*rac1 pdc1*^{crg1}	*a2b4 rac1*::*nour*^{R} *rho1*::P_{crg1}-*pdc1*-*cbx*^{R}	This study
Δ*rac1 pdc1*^{nar1}	*a2b4 rac1*::*nour*^{R} *rho1*::P_{nar1}-*pdc1*-*cbx*^{R}	This study
FB1Δ*cla4*	*a1b1 cla4*::*hyg*^{R}	26
Δ*cla4 pdc1*^{nar1}	*a1b1 cla4*::*hyg*^{R} *pdc1*::P_{crg1}-*pdc1*-*cbx*^{R}	This study
AB33	*a2bE2* Δ[$b2^I$ $bW2^V$]::[P_{nar1}*bW2* P_{nar1}*bE1ble*]	5, 53
AB33 *rho1*^{crg1}	*a2bE2* Δ[$b2^I$ $bW2^V$]::[P_{nar1}*bW2* P_{nar1}*bE1ble*]*rho1*::*Pcrg1-rho1-hyg*^{R}	This study
AB33 *pdc1*^{crg1}	*a2bE2* Δ[$b2^I$ $bW2^V$]::[P_{nar1}*bW2* P_{nar1}*bE1ble*] *pdc1*::P_{crg1}-*pdc1*-*hyg*^{R}	This study
SG200	*a1mfa2bW2bE1 ble*^{R}	34
GFP-rho1	*a1mfa2bW2bE1 ble*^{R} P_{otef}-*GFP-rho1 cbx*^{R}	This study
RFP-pdc1	*a1mfa2bW2bE1 ble*^{R} P_{otef}-*RFP-pdc1 cbx*^{R}	This study
d132	*a1a2b1b2*	24
d132Δ*rho1*	*a1a2b1b2 rho1 rho1*::*cbx*^{R}	This study
d132Δ*pdc1*	*a1a2b1b2 pdc1 pdc1*::*cbx*^{R}	This study
Plasmids		
pUM-*rho1*	P_{gap}-*rho1 cbx*^{R}	This study
pOtef-*rac1*	P_{otef}-*rac1 cbx*^{R}	This study
pYES-*pdc1*	pYES2.1/V5-His-TOPO (Invitrogen), P_{GAL}-*pdc1*	This study

The cDNA library of *U. maydis* cloned in pGADT7, as prey vectors, was generously provided by S. Klosterman (University of Georgia). The library was produced from strain 1/9, a *uac1* a1 strain that constitutively grows as filaments on rich media and was used for analyses of the Ubc2 adaptor protein (21). The yeast haploid strain Y187 was transformed with each respective bait plasmid and selected on SD/−Trp medium plates. The cDNA library in pGADT7 was obtained already transformed into yeast haploid strain AH109. Mating reactions were set up between two haploid strains containing bait vector and prey vector, respectively. After mating, the cells were plated on QDO (SD/−Trp/−Leu/−His/−Ade) or TDO (SD/−Trp/−Leu/−His) to select for potential protein interactions.

Colonies growing on QDO, which offers more stringent selection than TDO, were subsequently streaked on another QDO plate that contained α-D-X-Gal (α-D-5-bromo-4-chloro-3-indolyl-β-D-galactopyranoside) to test the activity of α-D-galactosidase, which is another marker gene under regulation of the Gal4 protein. Cells turning blue would indicate that the α-D-galactosidase expression was activated and that the Gal4 protein was active. Colonies that turned blue on a QDO/α-D-X-Gal plate were then inoculated in liquid culture for plasmid isolation. The isolated plasmids, which were pGADT7 vector containing cDNA fragments from the library, were then transformed into DH5α bacterial strains and selected on ampicillin plates since pGADT7 has an ampicillin resistance gene as a selectable marker.

pGADT7 vectors containing cDNA fragments were then isolated from bacte-

ria and the insert sequence was analyzed by using AD5′ or AD3′ primers that flank the cloning site of the pGADT7 vector. The sequences obtained were used in BLASTn searches against the *U. maydis* genome database (MIPS *U. maydis* database [http://mips.gsf.de/genre/proj/ustilago/]) to identify the genes.

Directed yeast two-hybrid experiments were also conducted in which the bait was specifically selected to test for interaction with a particular prey. This method was also performed to confirm initial positive interactions; genes identified initially as interacting with a particular bait protein were cloned into the bait vector and subjected to yeast two-hybrid with the original bait target now cloned into the prey vector. Specifically, the *pdc1* open reading frame (ORF) was amplified and cloned into the pCR2.1 TOPO vector (Invitrogen). The cloned *pdc1* ORF was then excised and inserted into pGADT-1 and pGBKT-7 at the EcoRI site to create pGAD-Pdc1 and pGB-Pdc1, respectively. This same technique was also used to generate pGAD-Rho1 and pGB-Rho1. The pGAD-Cdc24 was recovered from the yeast two-hybrid cDNA library (21).

For directed two-hybrid assays, bait and prey plasmid constructs were introduced into *S. cerevisiae* strain AH109 (BD Biosciences) by cotransformation. Growth was assessed after 5 days on both −Trp/−Leu/−His SD medium supplemented with 10 mM 3-amino-1,2,4-triazole (3-AT; Sigma, St. Louis, MO) and −Trp/−Leu/−His/−Ade synthetic dropout medium. The latter medium was overlaid with α-X-Gal (BD Biosciences). The amount of 3-AT used was determined by assessing the growth of positive controls in the presence of 10 and 30 mM concentrations of 3-AT; 30 mM was deemed slightly inhibitory to the growth of positive controls, whereas both concentrations were fully inhibitory to negative control strains. Therefore, 10 mM 3-AT was used.

In vitro coimmunoprecipitation. From among potential interactors of Rho1 initially indicated by yeast two-hybrid analyses, in some cases, coimmunoprecipitation (BD Matchmaker Co-IP kit; Clontech Laboratories, Inc., Mountain View, CA) was also used as confirmation. All proteins used for coimmunoprecipitation were synthesized via in vitro translation reactions using [^{35}S]methionine to label protein products in accordance with the TNT coupled reticulocyte lysate systems protocol (Promega).

Vector construction. The pYES-*pdc1* expression vector used in yeast complementation experiments was generated by cloning the *pdc1* ORF into pYES2.1/V5-His-TOPO (Invitrogen). This vector was sequenced for accuracy before transformation of the L6247 yeast strain. Genetic manipulations, including deletions and promoter replacements in *U. maydis*, were accomplished through homologous recombination as described previously (6). The *pdc1* and *rho1* constructs were created by using the SfiI technique (6). Approximately 1-kb fragments upstream (up-flank) and downstream (down-flank) of the gene of interest were amplified and used as flanking regions. For promoter replacement constructs, *rho1* and *pdc1* ORFs were substituted as the down-flanks. The *rho1* deletion construct was generated by using a fusion PCR method as described previously (46, 58). The 3′ end of the up-flank and the 5′ end of the down-flank are complementary to the 5′ and 3′ regions of the carboxin resistance cassette, respectively. Knockout and promoter replacement constructs were digested with restriction endonucleases, purified, and used to transform *U. maydis* protoplasts (6). Transformants with the desired replacements were identified and confirmed by PCR and/or Southern blot hybridization experiments (40). Expression levels in promoter-replacement cells for specific genes were determined by reverse transcription-PCR (RT-PCR) (40). The *rac1* expression vector was constructed by amplifying and cloning the *rac1* ORF into pCR2.1 TOPO. The *rac1* ORF was then excised and cloned after the P_{otef} promoter into the XmaI and NotI sites of the p123 vector (53) to provide constitutive expression. *U. maydis* expression vectors were linearized by using SspI before *U. maydis* was transformed and recombination occurred at the *ip* locus, with selection for carboxin resistance (5).

RNA isolation and expression analysis. RNA isolation from *U. maydis* was carried out by using the TRIzol reagent protocol from Invitrogen (Invitrogen) with minor modifications. *U. maydis* cells were grown on agar plates of appropriate medium for 3 to 5 days. The cells were scraped off the plate and homogenized with a mortar and pestle in liquid nitrogen. Approximately 100 mg of homogenized cells and 1 ml of TRIzol reagent were used for further RNA extraction steps. Extracted RNA samples were treated with DNase I (Epicentre) before carrying out RT-PCR. RT-PCR was done by using the RETROscript kit (Ambion).

Cell viability, growth rate, mating, confrontation assays, and plant infection. Cell density in liquid culture was measured by using a spectrophotometer. The optical densities were determined for cells grown in liquid medium at 28°C with shaking (200 rpm) for 48 h (with a change of the medium at 24 h). The ATP concentration was measured by using a BacTiter-Glo kit (Promega, Madison, WI). This method was accomplished by mixing 100 μl containing 10^6 cells and 100 μl of BacTiter-Glo reagent in an opaque-walled, 96-well plate. The reaction was incubated at room temperature for 5 min. Luminescence was recorded by using a plate-luminometer (Promega). To determine growth rates, *U. maydis* cells were allowed to reach exponential growth phase in YEPS broth. The cells were collected, washed once with fresh YEPS, and then resuspended in fresh YEPS. Afterward, 10^9 cells were transferred into 10 ml of fresh YEPS, and the optical density was determined every 2 h for 10 h. All data were analyzed by using Microsoft Excel. Mating and confrontation assays were done on charcoal plates as previously described (11). Plant infection using 8-day-old Golden Bantam corn seedlings was achieved as previously described (11).

Staining and microscopy. Staining of *U. maydis* cell walls, nuclei, and vacuoles was achieved by treating 6-μl portions of freshly grown cells with 1 μl of 10 mg of calcofluor/ml (2 μg/ml; Fluorescent Brightener 28; Sigma), Syto-11 (5 nM), or CellTracker Blue CMAC (100 μM), respectively (29, 45). Syto-11-stained and green fluorescent protein (GFP)-tagged cells were visualized by using a fluorescein isothiocyanate-filter set and a Nikon or Zeiss Axiophot DIC fluorescence microscope. For calcofluor- and CMAC-stained cells, a UV filter set was used for visualization. Images were taken by using either Volocity 4.1 or MetaMorph imaging software. Photoshop CS was used to process the images.

RESULTS

Rho1 possesses substantial amino acid sequence identity to Rho1 proteins and is essential for normal cell growth in *U. maydis*. Initial analysis of the *U. maydis* genome sequence revealed four genes predicted to encode Rho-like proteins: the previously described genes um10663, *rho2* (um02494), and *rho3* (um04070) (26, 55), and an additional Rho-like protein, *rho1* (um05734). The predicted Rho1 (um05734) bears the signature motifs shared by other Rho-GTPases. These include the GTP-binding site motif A (p-loop) at the N terminus (amino acids 12 to 19) and the prenylation site (CAAX box, amino acids 191 to 194) preceded by a polybasic group at the C terminus (8, 55). A blastp analysis using the predicted amino acid sequence of Rho1 (um05734) against the nonredundant database at NCBI (www.ncbi.nlm.nih.gov) yielded as highest hits, either hypothetical proteins with RhoA-like domains or those already identified as Rho1 homologues. When we compared the predicted sequence of Rho1 with those of Rho proteins from *Schizosaccharomyces pombe*, *S. cerevisiae*, *Cryptococcus neoformans*, and *Homo sapiens*, a high degree of similarity was found in each case with the respective Rho1 for these organisms (Fig. 1A).

To gain more insight into the functions of Rho1, we decided to carry out deletion experiments with haploid *U. maydis* cells. After several unsuccessful attempts, we elected to delete one copy of the gene in diploid cells. Successful deletion of one copy of the *rho1* gene only in diploid cells suggested that this gene might be essential. This observation prompted us to use an inducible promoter of a carbon-source regulated gene, (*crg1*) to study Rho1. The expression levels of the gene under different growth conditions (i.e., induced with arabinose or repressed with glucose) were confirmed by RT-PCR (see Fig. S1 in the supplemental material). Haploid strains in which the *crg1* promoter drove the expression of *rho1* displayed growth defects when the strains were grown on glucose-containing yeast extract-peptone-dextrose (YPD) medium, where the gene would be repressed (Fig. 1B). In contrast, when *rho1^{crg1}* cells were placed on arabinose-containing yeast extract-peptone (YPA) medium with the gene highly expressed (see Fig. S1 in the supplemental material), their growth was comparable to wild-type cells (Fig. 1B). Similar results were observed in the corresponding broth media. Cell density of *rho1^{crg1}* strain was significantly less than wild type (roughly 0.38%) after 48 h in YPD broth. In addition, we monitored the health status of

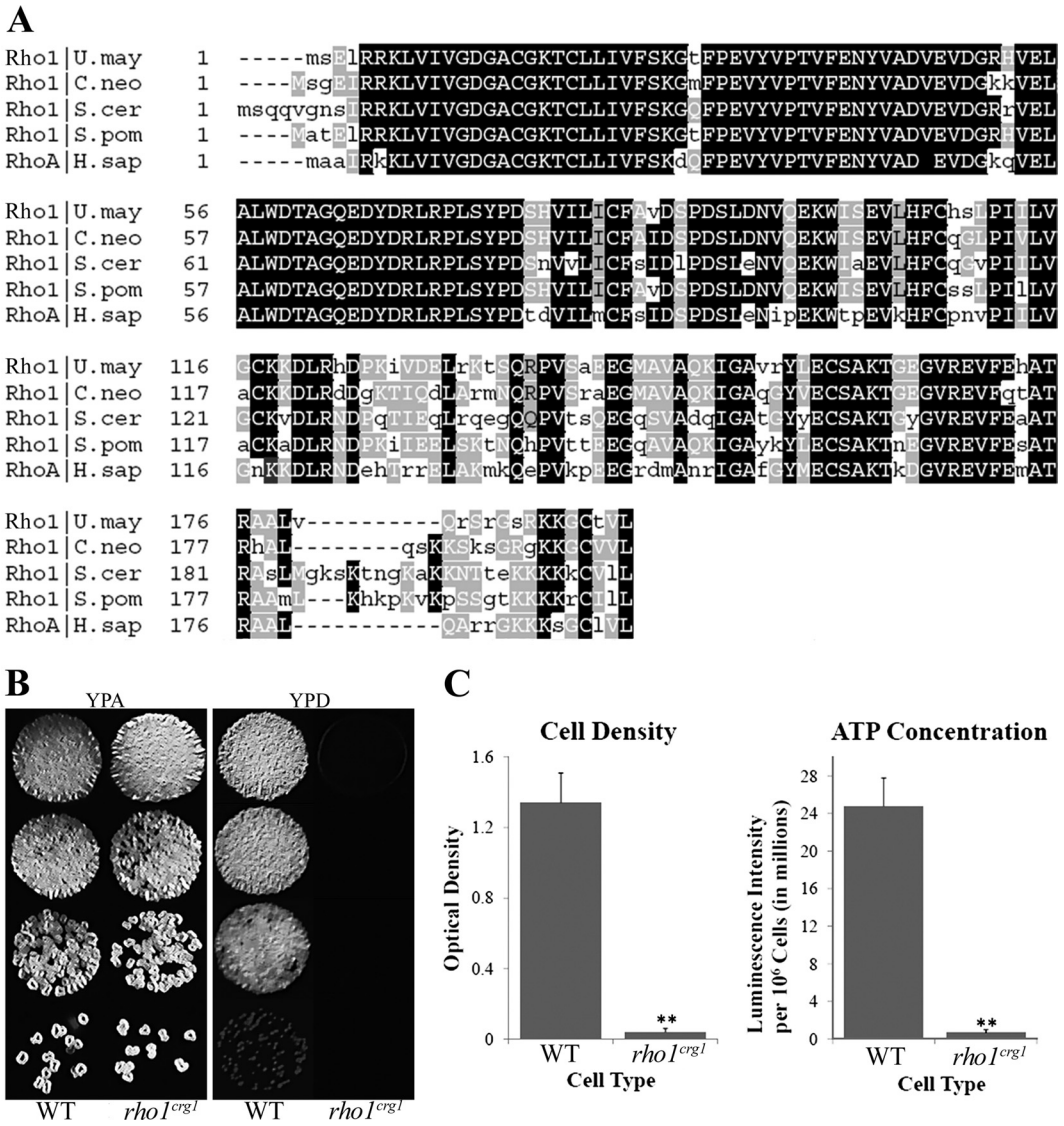

FIG. 1. Rho1 is highly conserved and essential for growth. (A) Protein sequence alignment indicates that Rho1 shares high similarity to Rho1 from other fungi and human RhoA. (B) *rho1*^{crg1} cells grow to the same degree as wild type on arabinose (YPA) media, but they grow poorly on glucose (YPD) media. (C) Similarly, cell density and ATP concentration of the *rho1*^{crg1} cells are significantly lower than those of wild-type cells when grown in glucose media. WT, wild type.

rho1^{crg1} cells by using the BacTiter-Glo cell viability assay. This assay determines the health status of cells in culture by measuring ATP concentration and with an assumption that healthy cells generate more ATP than dying cells generate. As expected, we observed ATP production dropped to less than 1/100 of that in the wild type for *rho1*^{crg1} grown in glucose for 48 h (Fig. 1C). These data further support the notion that *rho1* is required for normal cell growth.

Rho1 depletion results in aberrant morphologies prior to cell death. Microscopically, the cellular morphologies of cells depleted for Rho1 were visually distinct from that of wild type. Many cells exhibited multiple-budding or clustered phenotypes (Fig. 2A). Some cells displayed a unipolar protrusion (Fig. 2A), a characteristic of constitutively active Rac1 (29). To gain insight into the morphological defects that subsequently result in cell death when *rho1* is turned off (or down), we used stains that are specific for cell wall (calcofluor), vacuoles (CMAC), and nuclei (Syto-11) to examine *rho1*^{crg1} cells grown in glucose-rich YPD broth. Using calcofluor stain, we noticed that the cell clusters contained only single cross walls separating compartments (Fig. 2A). We also observed that chitin deposition seemed more concentrated around the mother cell and at the vacuolated end. DNA staining with SYTO-11 revealed that the compartments in cell clusters each contained a nucleus (Fig. 2B). In addition, cells lacking Rho1 also contained numerous small or single abnormally large vacuoles (Fig. 2C). In contrast, *rho1*^{crg1} cells grown in YPA broth resemble wild-type cells in all aspects (see Fig. S2 in the supplemental material).

Overexpression of *rho1* leads to mating-type-dependent reduction in mating. Rho1 protein has been implicated in controlling filamentation in both filamentous and dimorphic fungi. In *Fusarium oxysporium*, a *rho1*-null strain is incapable of

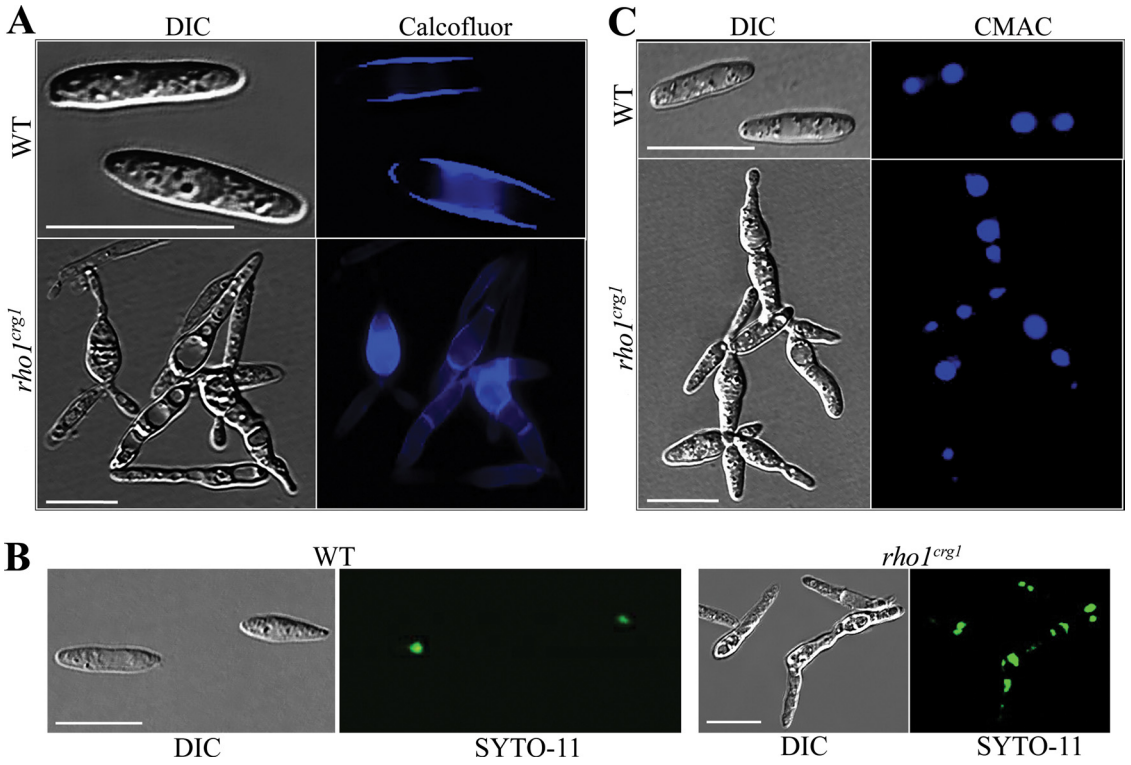

FIG. 2. Rho1-depleted cells show abnormal morphologies. Rho1^{crg1} cells growing in YPD media are more branching than wild-type cells. Unlike wild-type cells, Rho1-depleted cells contain multiple cross walls (A; stained with calcofluor), and each compartment contains a single nucleus (B; stained with Syto-11). (C) In addition, such cells contain more vacuoles than wild-type cells (stained with CMAC). DIC, differential interference contrast; WT, wild type. Scale bars, 10 μm.

maintaining hyphal growth on solid medium (30). However, unlike *F. oxysporium*, overexpression of *rho1* in *U. maydis* (see Fig. S3C in the supplemental material) led to mating deficiency. For these studies, we used *U. maydis* strains that carry plasmids bearing *rho1* fused to the *gap* promoter, pUM-*rho1*. Haploid cells carrying the pUM-*rho1* expression vector tend to grow more slowly than haploid cells carrying the pUM vector on plates (see Fig. S3A in the supplemental material), but these differences in growth were not statistically significant (see Fig. S3B in the supplemental material). Mixtures of strains bearing pUM-*rho1* showed marked reductions in aerial hyphae formation in comparison to wild-type strains 1/2 and 2/9 (Fig.

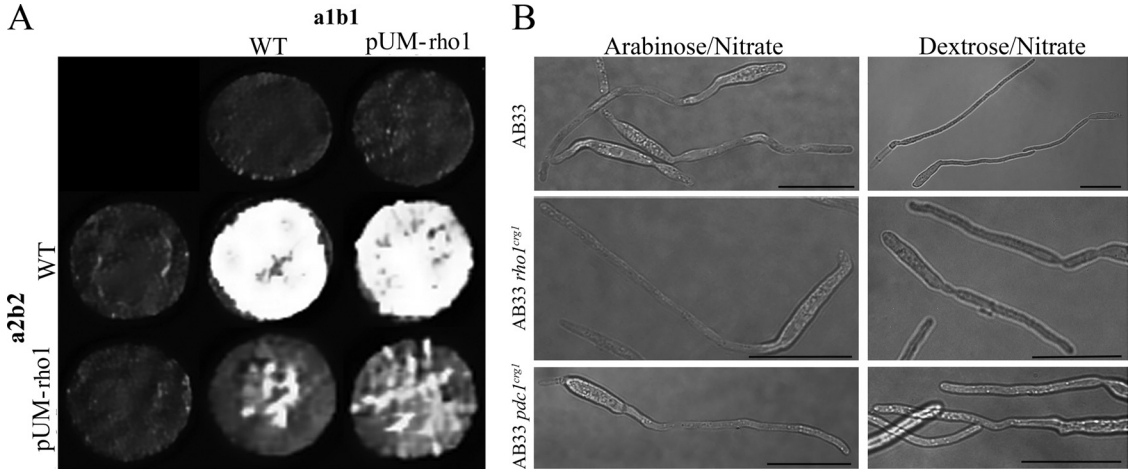

FIG. 3. Overexpression of *rho1* hampers filament formation. (A) Mating between strains that carry *rho1* overexpression vector (pUM-*rho1*) is less filamentous than the mixtures of wild-type cells of opposite mating-type. Interestingly, reduction in mating is mating-type dependent, since mating between wild-type *a1b1* and *a2b2* strains bearing pUM-*rho1* is more severely reduced than mating between wild-type *a2b2* and *a1b1* strains bearing pUM-*rho1*. (B) Control of mating filaments by Rho1 and Pdc1 appears to be upstream of the *b* mating locus. We observed that neither up- nor downregulation of *rho1*or *pdc1* affected filament formation in strain AB33 once the *b* locus was induced. WT, wild type.

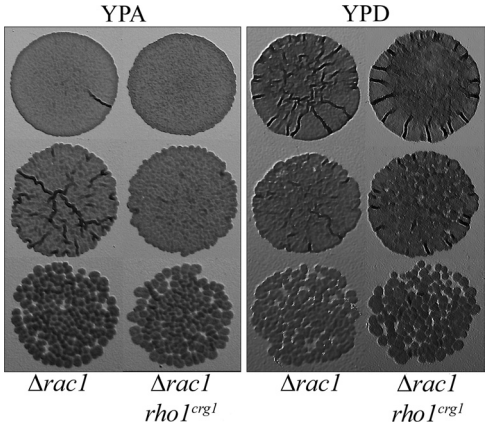

FIG. 4. Knockdown of *rho1* in Δ*rac1* mutant does not lead to cell death. *rho1*^{crg1} Δ*rac1* cells grow as well as Δ*rac1* cells on YPA. Strikingly, *rho1*^{crg1} Δ*rac1* cells are also able to grow on YPD, where Rho1 is depleted.

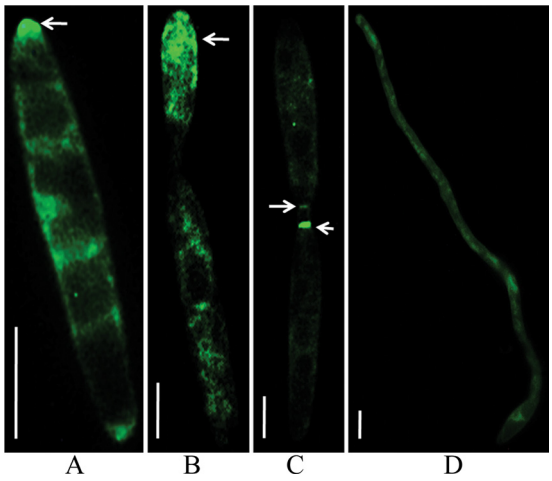

FIG. 5. Rho1 localizes at the growing tip and at the septa in wild-type cells. In vegetative and filamentous cells (panels A and D, respectively), GFP-Rho1 is dispersed throughout the cell with a slightly more localized appearance at the growing tip of nonfilamentous cells (panel A). In contrast, in dividing cells (panels B and C), GFP-Rho1 is more concentrated in the growing daughter cell initially (B), but then localizes (arrows) at the septation area during cytokinesis (C). Scale bars, 10 μm.

3A). Mixtures of compatible wild-type strains with *rho1* overexpression strains also showed reduction in mating. Moreover, mating reduction was more pronounced when *rho1* was overexpressed in the *a2b2* mating-type background (Fig. 3A; also see Fig. S3C in the supplemental material for confirmation of *rho1* overexpression). Several studies have observed similar, as-yet-unexplained effects of mating-type background on phenotypes associated with deletion or overexpression of genes in *U. maydis* (26, 46). The reduction in mating could be due to interference with the cell fusion process controlled by the *a* mating locus or to interference with filament induction controlled by expression of the *b* locus. However, we did not observe a reduction in filamentation when *rho1* was overexpressed, while the *b* locus was simultaneously induced (i.e., in the AB33 background; Fig. 3B). AB33 normally grows filamentously in nitrate-containing medium due to induced expression of its *b* mating-type locus that encodes an active fusion bE/bW transcription factor (54). Similarly, we also noticed that AB33 cells lacking *rho1*, although eventually nonviable, are still filamentous in nitrate-containing medium, where active fusion bE/bW transcription factor is expressed (Fig. 3B). In addition, confrontation assays between wild-type 1/2 and *rho1*-overexpressing 2/9 cells displayed fewer and shorter filament extensions (see Fig. S3D in the supplemental material). These data suggest that *rho1* is required for filamentation in a dosage-dependent manner. Overexpression of *rho1* seems to impose a negative effect on the *a* locus, possibly reducing the response to pheromone. In contrast, *rho1* does not seem to have any effect on filament formation once *U. maydis* cells have committed to filamentation. This observation is consistent with GFP-Rho1 expression in the SG200 strain (see below and Fig. 5), where the fluorescent protein is found diffusely in filaments rather than concentrated at budding tips or septa (as seen in budding cells).

Lethality due to Rho1 depletion requires Rac1. It has been reported that the small G proteins Rac1 and RhoA have opposite roles in mammalian systems (8, 36). In addition, in *U. maydis*, overexpression of *rac1* leads to filaments consistent with *b* induction, whereas deletion of *rac1* eliminates filamentation altogether (25). As mentioned above, we observed that Rho1 also modulates *b*-induced filament formation. Accordingly, we anticipated that Rac1 and Rho1 might participate in the same pathway(s). To test this hypothesis, we decided to replace the *rho1* promoter with the *crg1* promoter in the *rac1*-null strain. Surprisingly, the Δ*rac1 rho1*^{crg1} strain grew on YPD (Fig. 4). Knockdown or overexpression of *rho1* in the Δ*rac1* background strain had no discernible phenotype from that of the Δ*rac1* mutant alone.

Rho1 localizes at the growing tip and at the septum during cytokinesis. In an attempt to further understand the function(s) of Rho1, we tagged the N terminus of Rho1 with the GFP (Fig. 5) (47). Nondividing cells expressing GFP-Rho1 displayed a somewhat punctate appearance but with noticeably more fluorescence (i.e., fusion protein) concentrated at the growing tip. Similarly, in filamentous cells GFP-Rho1 was also dispersed all over the cell. In contrast, in dividing cells, GFP-Rho1 seemed to localize more at the tip of the newly emerging daughter cell. As cell division progressed, GFP-Rho1 accumulated at the two-septum structure that delineates mother and daughter cells. This suggests that Rho1 activity is both temporally and spatially regulated in *U. maydis*.

Interaction between Rho1 and a 14-3-3ε homologue suggests they may share a commonality of functions. By inference from the Rho1 localization data, we speculated that other proteins might be involved in the spatial-temporal regulation of Rho1. Thus, we decided to use yeast two-hybrid analysis to screen for proteins that interact with Rho1. From yeast two-hybrid analysis, we found a number of potential interactors for Rho1 (see Table S1 in the supplemental material). Importantly, yeast two-hybrid data suggested that Rho1 interacts with Cdc24, a RhoGEF that has also been shown to function as a GEF for Rac1 (29). Although no potential GAP or GDI was detected in the screen, yeast two-hybrid analysis identified a *U. maydis* 14-3-3 homologue as an interactor of Rho1 as well. For

a subset of genes identified as showing interaction, as indicated by growth on QDO stringent medium, the interactions were confirmed by directed yeast two-hybrid analysis and experiments in which the bait and prey were switched. Further, interactions for Rho1 with Cdc24, Smu1 (a Ste20 homologue) (46), Ump2 (a high-affinity ammonium transceptor; um05889), and PTEN (um03760, related to phosphatidylinositol-3,4,5-trisphosphate 3-phosphatase) were also confirmed via in vitro coimmunoprecipitation (see Fig. S4 in the supplemental material). In further support of the interaction between Rho1 and the 14-3-3 homologue, in silico sequence analysis revealed a 14-3-3 protein binding site on Rho1. Since 14-3-3 proteins had been shown to regulate a GEF of Rho-GTPases (59), we speculated that *U. maydis* 14-3-3 might be involved in the regulation of Rho1 localization.

***U. maydis* 14-3-3 protein is functionally conserved and is essential in *U. maydis*.** When we scanned the *U. maydis* genome for putative 14-3-3 genes, only one ORF (um01366) was predicted to encode a 14-3-3-like protein. Although another predicted protein (um11124, updated as um04193.2) has an InterPro match (IPR000308) to a 14-3-3 domain, the protein does not resemble a 14-3-3 overall and deletion of um11124 did not result in any discernible phenotype (data not shown). An attribute of 14-3-3 proteins is their binding of phosphorylated proteins (50); hence, we named the *U. maydis* 14-3-3 homologue Pdc1 (for phosphorylation-domain coupling protein [10]). Pdc1 is comprised of two 14-3-3 signature motifs at amino acids 43 to 53 and amino acids 215 to 234. Pdc1 shares high similarity with the 14-3-3 homologues identified in *C. neoformans* (96%) and *S. cerevisiae* (82%) and with the *H. sapiens* 14-3-3ε variant (79%) (Fig. 6A). The protein has since also been named Bmh1 (32) due to its high amino acid similarity to the corresponding protein in *S. cerevisiae*. To confirm the predicted function of the *U. maydis* 14-3-3 homologue, we tested whether it is able to rescue the phenotype of the respective yeast mutant; we introduced *pdc1*, on plasmid pYES-*pdc1*, into *S. cerevisiae* L6247(Δ*bmh1 bmh2*). This mutant is normally unable to grow at 37°C (G. Fink, unpublished data) and does not grow well on galactose as the sole carbon source. However, when *U. maydis pdc1* was expressed from the *GAL1* promoter, the temperature-sensitive growth defect of the mutant was at least partially alleviated, as evidenced by improved growth of the transformed double mutant at 37°C (see Fig. S5 in the supplemental material).

As mentioned earlier, from yeast two-hybrid analysis, Pdc1 interacts with Rho1 (and a large number of other proteins are potential interactors with Pdc1 as well [see Table S1 in the supplemental material]). In addition, *pdc1* also seems to localize in the same areas as *rho1* does (see Fig. S6 in the supplemental material). Like GFP-Rho1, RFP-Pdc1 transiently localizes at the growing and/or dividing tip. Nondividing cells expressing RFP-Pdc1 displayed a somewhat punctate appearance but with noticeably more fluorescence (i.e., fusion protein) concentrated at the growing tip. In addition, in dividing cells, RFP-Pdc1 seemed to localize more at the tip of the newly emerging daughter cell. This suggests that, like Rho1, Pdc1 activity is both temporally and spatially regulated in *U. maydis*. This lends more supporting evidence to our hypothesis that Pdc1 is involved in the temporal-spatial regulation of Rho1.

As with *rho1*, we were only able to disrupt one copy of *pdc1* in diploid *U. maydis* cells, and deletions in haploid strains could not be obtained. Transformants of the *U. maydis* strain d132 were confirmed to contain a single-allele deletion, and such a strain was then used for maize infection (11). Teliospores produced from the maize infection did not generate any progeny that segregated the drug resistance marker (data not shown), thus supporting our previous observation that strains with *pdc1* deleted are nonviable. Similarly, haploid strains in which the carbon source-regulated P_{crg1} promoter or the nitrate reductase promoter, P_{nar1}, drove expression of *pdc1* displayed growth defects (Fig. 6B) when grown on YPD (i.e., where either promoter would be off; see Fig. S7 in the supplemental material). In contrast, when cells were placed on YPA or $MMNO_3$ medium, *pdc1* promoter-replaced cells grew comparably to wild-type cells (Fig. 6B). Further, in liquid YPD (i.e., repressive) medium, the cell densities of *pdc1* promoter-replacement strains were significantly less than those of the wild type after 48 h (ca. 0.76% of the wild type; Fig. 6C). Similarly, the ATP content of the cells was less than 1/10 that of the wild type (Fig. 6C). These results suggest that Pdc1 is also essential for cell viability.

We noticed that cellular morphologies of Δ*pdc1* cells were visually distinct from those of wild-type cells. Noticeably, Δ*pdc1* cells demonstrated multiple budding and a highly filamentous phenotype within 20 h (Fig. 7A to C). Gradually, these cells displayed chromosomal condensation and selective-compartmental cell death. Calcofluor-stained cells revealed multiple cross walls (Fig. 7A). Unlike wild-type septation, these cross walls were devoid of secondary septa necessary for mother-daughter cell separation in *U. maydis*. Based on DNA staining, the compartments delineated by these cross walls all contained a nucleus (Fig. 7C). In addition, Pdc1-depleted cells also had many smaller vacuoles (Fig. 7B). Sustained *pdc1* knockdown led to hyperelongated cells with atypical, globular morphologies. Such cells formed globular capsulelike structures if maintained in YPD longer than 24 h (Fig. 7D). Eventually, these capsule structures detached and became free floating (Fig. 7E). The globular structures of prolonged Pdc1-deprived cells stained brightly with both calcofluor and Syto-11 (Fig. 7D). Similarly, the free-floating "capsules" also stained brightly with calcofluor and Syto-11 (Fig. 7E); however, they were not readily stained with CMAC (Fig. 7E), nor could we isolate such capsules in order to further characterize their viability or other features. These and other characteristics were not observed in *pdc1* promoter-replaced cells grown in permissive medium. *pdc1* promoter-replaced cells grown in permissive media resembled wild-type cells in all aspects, except that such cells showed a slightly more elongated cell morphology (see Fig. S8 in the supplemental material).

***pdc1* is not essential for aerial hyphae formation in *U. maydis*.** 14-3-3 functions have been associated with filamentous or pseudohyphal growth in *C. albicans* (37) and *Yarrowia lipolytica*. In *C. albicans* (30) and *Y. lipolytica* (16), strains with mutations in 14-3-3 proteins either develop abnormal filaments or fail to differentiate completely. To determine whether Pdc1 has any effect on aerial hyphae formation, we used $pdc1^{nar1}$ in otherwise wild-type-compatible mating types. The mating assay between such strains was conducted on nitrate containing medium. We did not notice any difference in aerial hyphae formation among such matings, where *pdc1* was overexpressed, and those between wild-

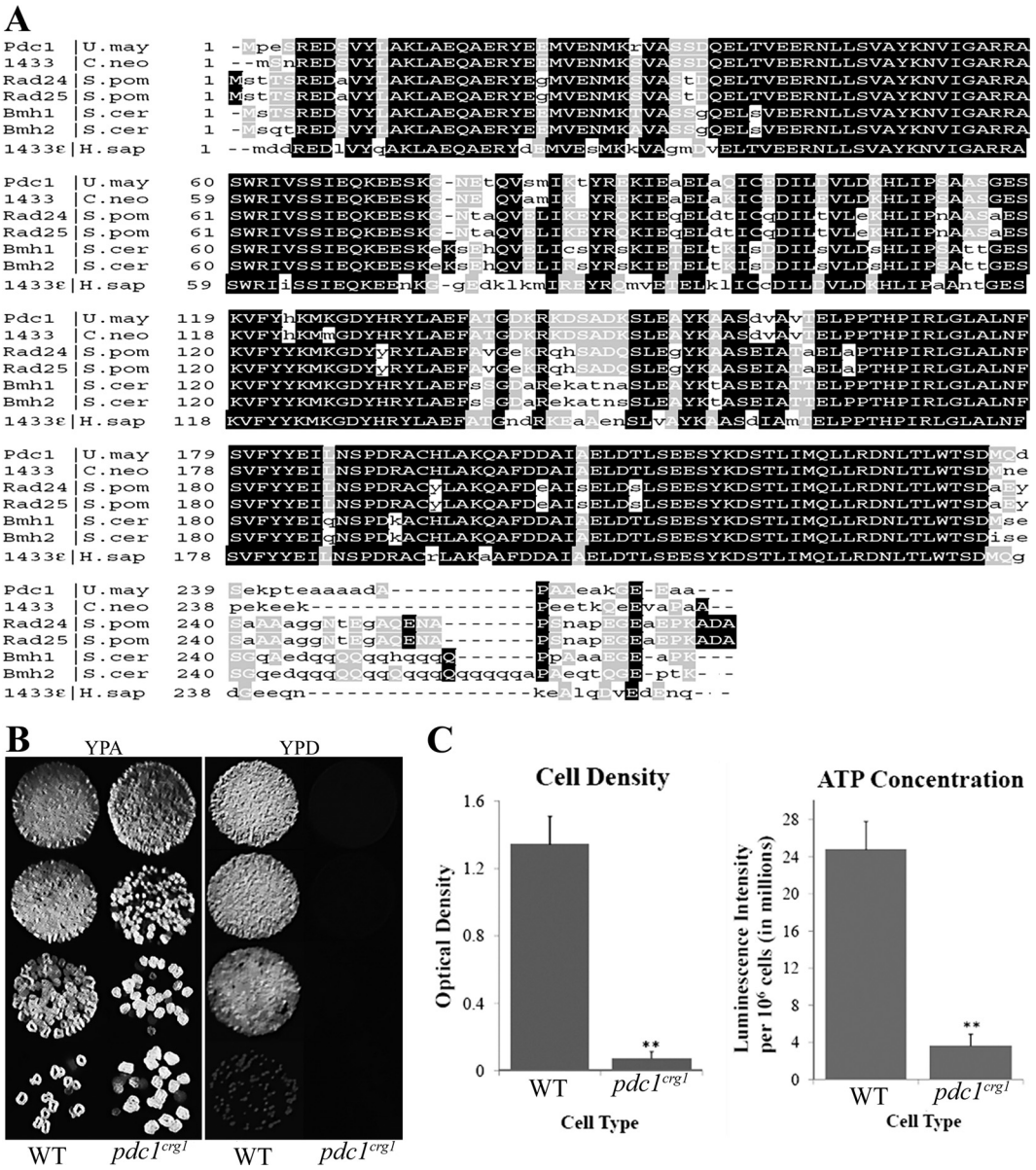

FIG. 6. Pdc1 has high amino sequence similarity to other 14-3-3 proteins, and it is essential for cell viability. 14-3-3 retains high sequence identity from humans to fungi. (A) Pdc1 shares highest similarity to the 14-3-3 of *C. neoformans*. *pdc1*^{crg1} cell growth is comparable to that of wild-type cells on YPA. (B) However, on YPD the *pdc1*^{crg1} cells are severely impaired in growth compared to the wild type. (C) Similarly, cell density and ATP amount (indicated as fluorescence units/10^6 cells) of the *pdc1*^{crg1} cells are significantly lower than those of wild-type cells when grown in glucose media. WT, wild type.

type strains. On the other hand, as with Δ*rho1* AB33 cells, *pdc1*^{crg1} AB33 cells were still able to generate mating filaments on minimal medium with dextrose and nitrate before ultimately dying (see Fig. S3E in the supplemental material) (Fig. 3B). This allows us to conclude that at least basal level Pdc1 activity is not essential for aerial hyphae formation.

Overexpression of *rho1* alleviates the *pdc1*-null phenotype, whereas deleting *rac1* or *cla4* suppresses *pdc1* depletion-induced lethality. Based on our data, we suspected that Rho1 and Pdc1 may participate in the same regulatory cascades in *U. maydis*. Therefore, we elected to replace the promoters of both *rho1* and *pdc1* with the *crg1* and *nar1* promoters, respectively, in a haploid strain. When we simultaneously repressed both *rho1* and *pdc1*, the cells died with the same characteristics as those of *rho1* knockdown cells (data not shown). Likewise, overexpressing *pdc1* did not rescue *rho1* knockdown cells and vice versa (data not shown). Intriguingly, however, although overexpressing *rho1* did not eliminate the eventual cell death from depletion of *pdc1*, it did block pseudohyphal formation induced by *pdc1* knockdown (Fig. 8A).

After realizing that Pdc1 could potentially be involved in the same regulatory cascade(s) as Rho1, we wanted to find out whether Rac1 could be a suppressor of lethality for Pdc1 as well. Thus, we decided to replace the *pdc1* promoter with

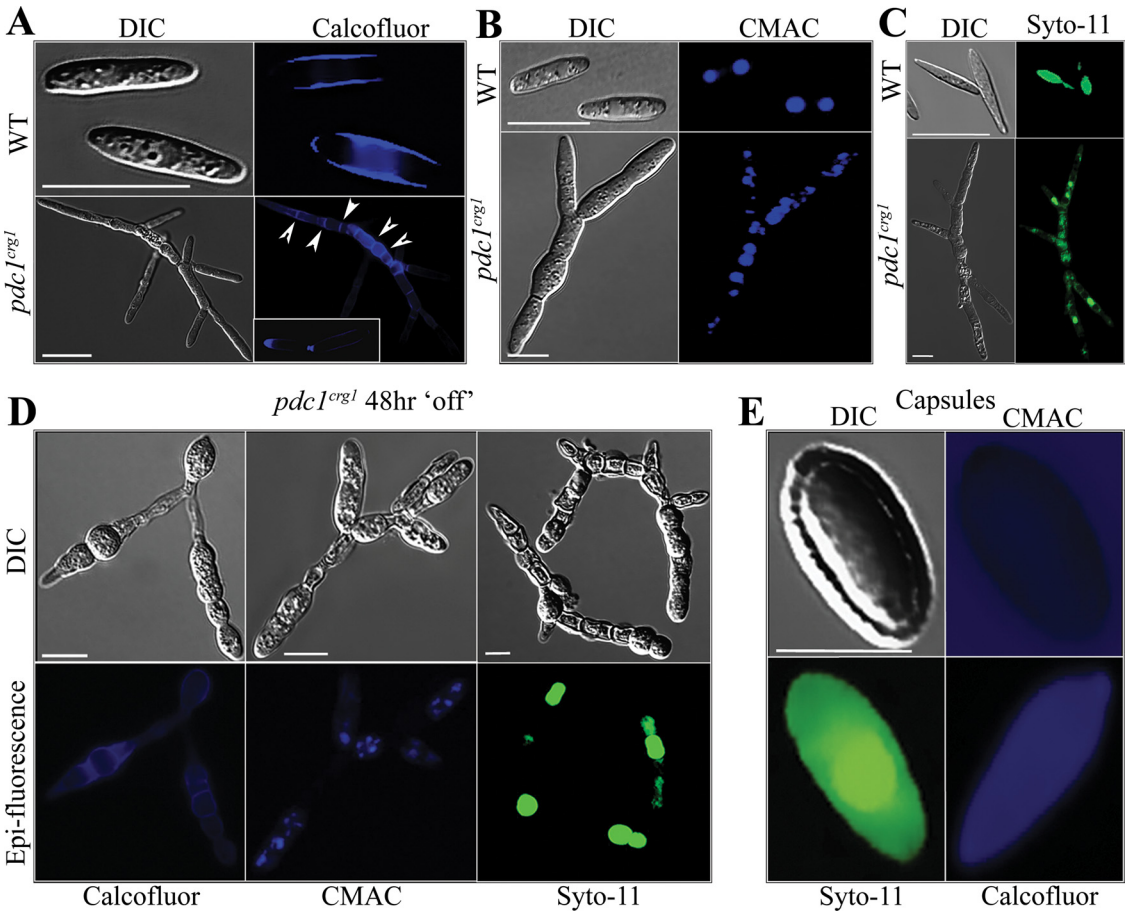

FIG. 7. Pdc1-depleted cells develop unusual morphologies. *pdc1*^{crg1} and *pdc1*^{nar1} cells growing in glucose-rich medium are branching, compared to wild-type cells. (Only results for *pdc1*^{crg1} cells are shown in the figure.) (A) Calcofluor-stained cells reveal numerous cross walls for Pdc1-depleted cells (arrows). In contrast, wild-type cells contain the primary and secondary septa consistent with dividing cells that will separate mother and daughter cells (inset). (B and C) In addition, Pdc1-depleted cells harbor numerous vacuoles (B) and nuclei (C) compared to the wild type. (D) Furthermore, prolonged Pdc1 depletion (24 to 48 h) leads to selective-compartmental cell lysis and capsule formation. The compartments where apparent lysis has occurred are devoid of chitin (D; calcofluor), vacuoles (D; CMAC), and nucleic acid material (D; Syto-11). (E) The capsules eventually detached into free-floating capsules. These free-floating capsules stained strongly with calcofluor and Syto-11, but not with CMAC. Scale bars: A to D, 10 μm; E, 5 μm. WT, wild type.

either P_{crg1} or P_{nar1} in the *rac1*-null strain. Strikingly, just like *rho1*^{crg1}, either *pdc1*^{crg1} or *pdc1*^{nar1} strains in the Δ*rac1* background were able to grow in repressive media (Fig. 8B and see Fig. S9A in the supplemental material). These cells had the same morphology as Δ*rac1* cells. However, unlike the case with *rho1*, overexpression of *pdc1* (see Fig. S9A in the supplemental material) in a Δ*rac1* background led to slower cell proliferation (Fig. 8B), suggesting possible roles for both *rac1* and *pdc1* in cell cycle regulation.

Lastly, we wanted to determine whether deleting the p21-activated kinase, Cla4, could also repress Pdc1 depletion-induced lethality. Cla4 protein has been shown to be the downstream effector of Cdc42 and Rac1 in *S. cerevisiae* (12) and *U. maydis* (26), respectively. Thus, we expected that the *cla4*-null mutant would also rescue Pdc1-depleted cells. To investigate this possibility, we replaced the *pdc1* promoter with the P_{nar1} promoter in the FB1Δ*cla4* background (see Fig. S9B in the supplemental material). As we suspected, when *pdc1*^{nar1}Δ*cla4* cells were placed on YPD medium, they grew just as well as had the Δ*cla4* mutant cells (Fig. 8C). Furthermore, *pdc1*^{nar1}Δ*cla4* cells displayed a more elongated phenotype than FB1Δ*cla4* in YPD (Fig. 8A).

DISCUSSION

Morphological transition in dimorphic fungi is a highly coordinated process. A successful transition requires the correct ensemble of different proteins that are necessary for polarity determination or cytokinesis. Recently, the Rho/Rac GTPases and 14-3-3 proteins have emerged as essential modulators of cell polarity, actin organization and cytokinesis (8, 33, 39). For example, Rac1 has been shown to regulate cell polarity, while Cdc42 regulates cytokinesis in *U. maydis* (29). In yeast and *F. oxysporum*, Rho1 has been suspected to play a crucial role in modulating the activity of chitin synthase, a core component of the cell wall biosynthesis machinery (30, 42). A *rho1*-null *F. oxysporum* is incapable of maintaining hyphal growth on solid medium (30). In mammalian systems, Rho/Rac-GTPases regulate lamellae formation. We have demonstrated here that

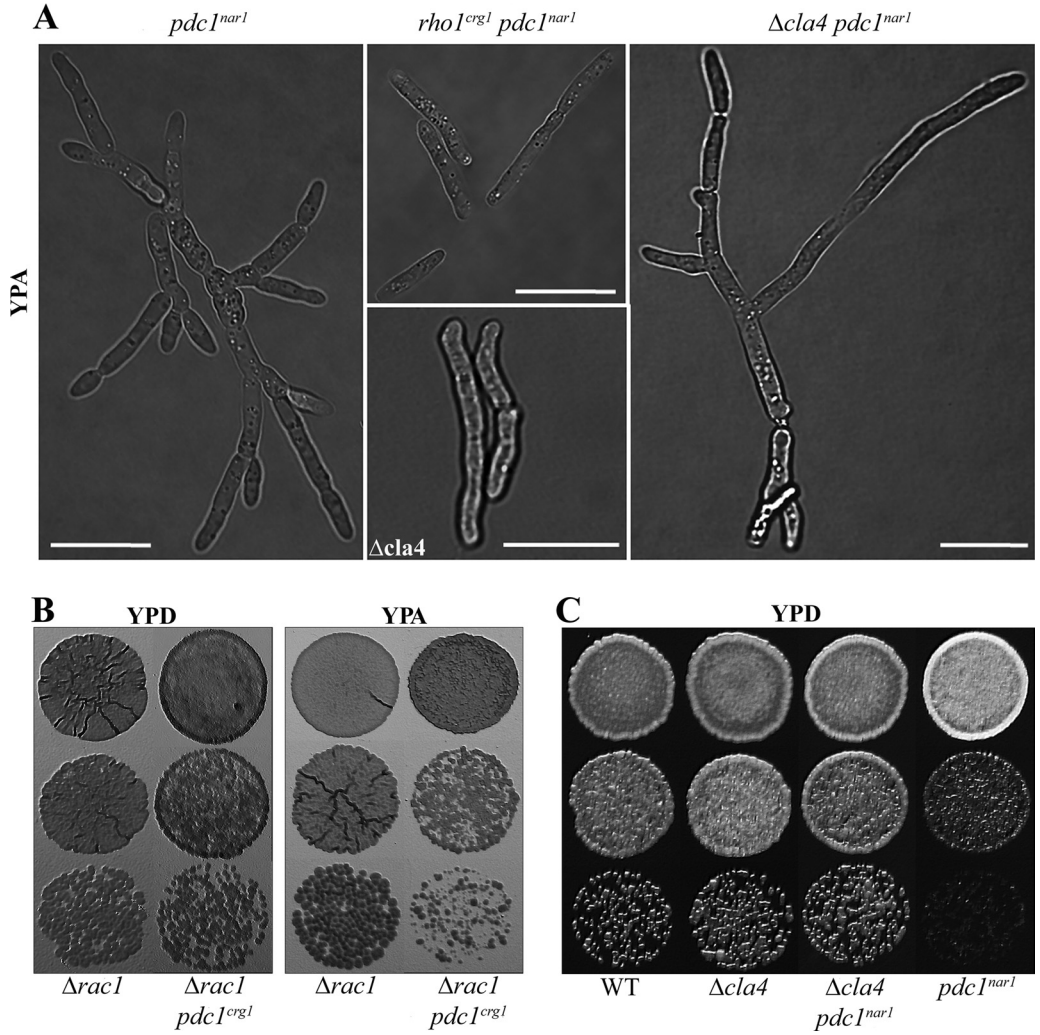

FIG. 8. Deletion of *rac1* or *cla4* and overexpression of *rho1* alleviate *pdc1* knockdown defects. (A) Simultaneous knockdown of *pdc1* and overexpression of *rho1* (*rho1*^{crg1} *pdc1*^{nar1}) eliminates pseudohyphal growth induced by Pdc1 depletion (*pdc1*^{nar1}). Deletion of *rac1* or *cla4* in *pdc1*^{crg1} or *pdc1*^{nar1} mutant background could reduce the growth defect displayed by *pdc1* knock-down. (B) Δ*rac1 pdc1*^{crg1} cells grow to the same degree as Δ*rac1* cells on YPD. Interestingly, Δ*rac1* cells fare better than Δ*rac1 pdc1*^{crg1} cells on YPA. In the Δ*cla4* background, with knockknown of *pdc1*, cells recover wild-type growth levels on YPD (C), and such cells possess a filamentous cell morphology (A) (Δ*cla4 pdc1*^{nar1}). Scale bars, 10 μm. WT, wild type.

another Rho-GTPase, Rho1, is also essential for both cytokinesis and cell polarity.

Like Rho-GTPases, 14-3-3 proteins (such as Pdc1) have been reported to possess pleiotropic roles. 14-3-3 proteins have been posited to regulate pseudohyphal growth in fungi. For example, in *S. cerevisiae*, 14-3-3 homologues Bmh1/Bmh2 regulate pseudohypha formation through the MAPK pathway (38). 14-3-3 proteins have also been implicated in controlling filamentation in other dimorphic fungi, especially in *C. albicans* (37) and *Y. lipolytica* (16). In these organisms, the extent of filamentous growth is proportional to the level of 14-3-3 protein expression (16). More importantly, 14-3-3 proteins have also been shown to be essential for viability in *S. cerevisiae* (38), *C. albicans* (9), and *S. pombe* (19). The cause of lethality in 14-3-3-null yeast and *C. albicans* has not been elucidated. However, 14-3-3 proteins have been shown to assist in the activation of Raf-1, an essential activator of the MAPK pathway that regulates cell proliferation in mammals (18). In *S. cerevisiae*, Bmh1 and Bmh2 also control G_1 transition (32). In contrast, for *U. maydis*, Pdc1 (also known as Bmh1 [32]) was additionally shown to be involved with cell cycle control of the G_2 transition (32) that was dependent on the phosphorylation state of the dual-specificity phosphatase Cdc25. However, there are no data showing whether or not altered expression of *cdc25* could rescue Pdc1-null cells. In *S. pombe* however, it has been shown that overexpression of a Cdc14 family phosphatase Clp1 could rescue the lethality induced by deletion of the gene encoding the 14-3-3 homologue, Rad24 (33). We propose here a model with possible pathways for Pdc1, Rho1, Rac1, and Cla4 in *U. maydis* that could help explain the role(s) of Rho1 and Pdc1 in cell growth and differentiation (Fig. 9).

Rho1 has been shown to be essential for cell viability in *S. cerevisiae* (28). Likewise, we demonstrated that *rho1* is essential for cell growth in *U. maydis*. It appears that *rho1* is the only

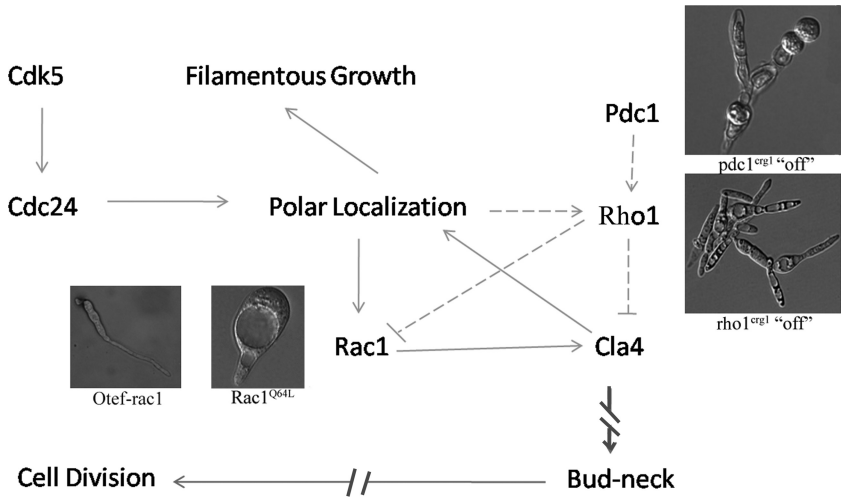

FIG. 9. Model for the concerted roles of Rho1 and Pdc1 in regulating cell separation, polarized cell growth, and filamentation. Rho1 and Pdc1 work upstream of Rac1 and the *b* mating locus. After activation of Rac1 by Cdc24, Rac1 sequesters Cla4 to the growing tip (29), subsequently leading to filamentous growth. It also has been demonstrated that the localization of Cdc24 is Cdk5 dependent (7). Cdk5 temperature-sensitive cells exhibit a phenotype similar to that of Pdc1-null cells. Rho1 and Pdc1 have antagonistic functions toward Rac1; this could be by interfering with Rac1 localization to the membrane. Alternatively, Rho1 could act negatively on Rac1 by sequestering Cdc24 or Cla4 away from Rac1. In vivo, Rho1 and Rac1 could compete for Cdc24. See the text for more in-depth discussion of the model. Solid arrows indicate a positive role on a protein or process confirmed experimentally in *U. maydis*; dashed arrows or bars indicate, respectively, a putative positive or negative role on a protein or process. Interrupted arrows indicate that a putative positive role that has not been investigated experimentally in *U. maydis*.

GTPase in *U. maydis* that is essential for cell viability. Knockout of *cdc42* or *rac1* alone does not result in cell death (29). However, *cdc42* and *rac1* double deletion or knockdown leads to cell death. A possible explanation for this is that, unlike Rho1, which controls both cytokinesis and polarity, Cdc42 and Rac1 separately regulate these two processes, respectively. We noticed that Rho1-depleted cells undergo lateral budding prior to cell death, indicative of a cell polarity problem. Moreover, GFP-Rho1 localizes at the growing cell tip, suggesting its involvement in polarity determination. Depletion of *rho1* does not affect nuclear division. However, depletion of *rho1* does affect vacuole formation and cell separation. When *rho1* expression is shut down, many cells failed to separate and formed clusters with cross walls. GFP-Rho1 also localized at the primary and secondary septa during cytokinesis. This implies that Rho1 is required for mother-daughter cell separation. Interestingly, both Rho1 and Rac1 share the same GEF, Cdc24, which is essential for cell viability (1). Taken together, we propose that Cdc42 and Rac1, which separately regulate their respective processes, may jointly assist Rho1 in governing cytokinesis and cell polarity determination.

All of the phenotypes associated with Rho1-null cells are also shared by Pdc1-depleted cells, and these have also been described previously (32). However, these phenotypes are delayed by about 24 h in Pdc1-null cells compared to Rho1-null cells. This suggests that Pdc1 acts upstream of Rho1, possibly acting as a scaffold. In addition, overexpression of *pdc1* and knockdown of *rho1*, or vice versa, does not rescue the lethality effect. However, overexpression of *rho1* does alleviate the pseudohyphal growth morphology of Pdc1 depletion. 14-3-3 proteins have been shown to modulate the localization of Rho and Rac through the interaction with a GEF (59). Interestingly, we have noticed that Rho1 does have a putative 14-3-3 binding site. Based on this, we argue that 14-3-3 could play an essential role in the localization of Rho1. This is consistent with our finding that RFP-Pdc1 localizes in a similar pattern to GFP-Rho1, although we did not observe localization of RFP-Pdc1 at the mother-daughter separation septa. We did see that Rho1 is temporally and spatially regulated in *U. maydis*. So, if *pdc1* were knocked down, Rho1 would be unable to stably localize at the appropriate site(s) to carry out its functions. This would subsequently lead to cell death.

An additional phenotype of cells depleted for Pdc1 for longer than 48 h is a capsulelike structure that has not been reported previously for *U. maydis*. These structures stained readily with calcofluor and Syto-11 (Fig. 7E), allowing detection of cell wall and nuclei, respectively. However, they were impervious to staining with CMAC (which stains vacuoles). Beyond these observations, we do not have additional understanding of their composition or function. On the other hand, it is intriguing to compare these to the bona fide capsule function in another basidiomycetous fungus, *C. neoformans.* Although the capsules of *C. neoformans* are structurally and likely functionally different than those of Pdc1-null cells, interestingly, capsule formation in *C. neoformans* is correlated with reduced transcription of the genes encoding the homologues of both 14-3-3 and Rac1 (27). Perhaps this provides a lead to follow in investigating a morphological structure similarly produced in *U. maydis* after extended periods of Pdc1 depletion.

Rho1 and Pdc1 are possible negative regulators of Rac1. In other systems, Rho1 has been shown to negatively regulate Rac1 either through GAP (36) or by interfering with Rac1 localization (8). In *U. maydis*, filamentation is mainly under the regulation of Rac1 (29) and products of the *b* mating locus (24, 43). Induction of *rac1* or the *b* mating locus leads to hyperfilamentation. In addition, it is posited that Rac1 is the activator of the p21-activating kinase, Cla4, because when Rac1 was stimulated in the *cla4* mutant no filamentation was observed

(25). We demonstrated here that both Rho1 and Pdc1, two essential proteins, are important regulators of the dimorphic switch in *U. maydis*. Prevention of either *rho1* or *pdc1* expression leads to nonpolarized filamentous growth and eventual cell death. Overexpression of *rho1* could also reduce filamentation. Reduction in filament formation was seen for both mating (Fig. 3) and confrontation assays (see Fig. S3D in the supplemental material) when *rho1* was overexpressed. Cells overexpressing *rho1* do form filaments, although much less, in confrontation assays, suggesting that they are still able to produce and sense pheromones. Interestingly, this effect was more pronounced when the partner in the mating assay was an a_2 strain. Such effects due to mating-type background have been observed previously for other genes in *U. maydis* (e.g., *smu1* [46] and *cla4* [26]), although the basis for such effects remains unclear. In addition, the control of filamentation by Rho1 seems to occur upstream of the *b* mating locus. This view is supported by the finding that when *rho1* (or *pdc1*) was repressed and the *b* mating locus was induced, the cells were still able to generate mating-like filaments. Taken together, this suggests that Rho1, Pdc1, and Rac1 may orchestrate filamentation via the same pathway(s) (Fig. 9). Moreover, based on our results, we think that Rho1 and Pdc1 function upstream of Rac1 and the *b* mating locus.

Additional evidence supporting the contention that Rho1 and Pdc1 are upstream of Rac1 is the fact that deletion of Rac1 rescued the lethality of Rho1 or Pdc1 depletion. It has been shown that cells carrying a constitutively active version of Rac1, $Rac1^{Q64L}$, promote delocalized isotropic cell wall extension and are not viable (29). Although cell morphology phenotypes differ significantly compared to $Rac1^{Q64L}$, Rho1-depleted cells also exhibit delocalized isotropic cell wall extension and reduced expression of *rho1* or *pdc1* mimics the outcome of constitutively active Rac1, i.e., concomitant cell death. Moreover, constitutively active Cla4, a Rac1 downstream effector protein, also leads to cell death (26). Interestingly, we observed that the *cla4* deletion mutant rescued the growth defects of Pdc1-null cells. This further supports the idea that Pdc1 and Rho1 participate in the Rac1-Cla4 regulatory pathway(s). Therefore, as shown in our model, negative regulation of Rac1 by Rho1 could be accomplished by direct and indirect means (Fig. 9). It has been shown that upon activation of Rac1 by Cdc24, facilitated by Cdk5 (7), Rac1 sequesters Cla4 to the growing tip (32). In addition, at the nonpermissive temperature, Cdk5 temperature-sensitive cells exhibit a phenotype similar to that of Pdc1-depleted cells (7). Thus, Rho1 could interfere with Rac1 activities by preventing Rac1 from localizing at the growing pole. Other possibilities for how Rho1 could indirectly act as negative regulator of Rac1 are by sequestering Cdc24 or Cla4 away from Rac1. Yeast two-hybrid analyses suggest possible interaction between Cdc24 and Rho1. As with Rho1, Cdc24-null cells are nonviable. In vivo, Rho1 and Rac1 could compete for Cdc24. On the other hand, Cla4 has been shown to localize at the bud-neck in *S. cerevisiae* (2). According to the GFP-Rho1 data, Rho1 also localizes (possibly with the help of Pdc1) at the bud-neck or in the septation area. Thus, it is a possibility that Rho1 is somehow involved with sequestration of Cla4 to the septation area and away from the growing tip and Rac1. In such cases, cells would then undergo budding instead of filamentation. Temporal-spatial regulation of Rho and Rac proteins is tightly coordinated by GAPs, GDIs, and possibly by 14-3-3 proteins (59), and there is also evidence of cross talk between Rho and Rac (8). Moreover, there seem to be feedback controls between Rho, GAP, GDI, and PAK as well (48). Such spatial and temporal regulation of Rho/Rac-GTPases might help explain the opposite roles of Rho1 and Rac1 in *U. maydis*.

ACKNOWLEDGMENTS

We thank David A. Myers for his constructive criticism of the manuscript. We also thank two anonymous reviewers solicited by the journal for their insightful comments and suggestions that improved the quality of the manuscript prior to its publication.

This study was supported, in part, by a grant from the Arts and Sciences Research Fund and by an IRIG-RIG from the Office of the Vice President for Research at the University of Louisville.

REFERENCES

1. **Alvarez-Tabarés, I., and J. Pérez-Martin.** 2008. Cdk5 kinase regulates the association between adaptor protein Bem1 and GEF Cdc24 in the fungus *Ustilago maydis*. J. Cell Sci **121:**2824–2832.
2. **Asano, S., J.-E. Park, K. Sakchaisri, L.-R. Yu, S. Song, P. Supavilai, T. D. Veenstra, and K. S. Lee.** 2005. Concerted mechanism of Swe1/Wee1 regulation by multiple kinases in budding yeast. EMBO J. **24:**2194–2204.
3. **Böhmer, C., M. Böhmer, M. Bölker, and B. Sandrock.** 2007. Cdc24 and the Ste20-like kinase Don3 act independently in triggering cytokinesis in *Ustilago maydis*. J. Cell Sci. **121:**143–148.
4. **Böhmer, M., T. Colby, C. Böhmer, A. Bräutigam, J. Schmidt, and M. Böker.** 2007. Proteomic analysis of dimorphic transition in the phytopathogenic fungus *Ustilago maydis*. Proteomics **7:**675–685.
5. **Brachmann, A., G. Weinzierl, J. Kämper, and R. Kahmann.** 2001. Identification of genes in the bW/bE regulatory cascade in *Ustilago maydis*. Mol. Microbiol. **42:**1047–1063.
6. **Brachmann, A., J. König, C. Julius, and M. Feldbrügge.** 2004. A reverse genetic approach for generating gene replacement mutants in *Ustilago maydis*. Mol. Genet. Genomics **272:**216–226.
7. **Castillo-Lluva, S., I. Alvarez-Tabarés, I. Weber, G. Steinberg, and J. Pérez-Martín.** 2007. Sustained cell polarity and virulence in the phytopathogenic fungus *Ustilago maydis* depends on an essential cyclin-dependent kinase from the Cdk5/Pho85 family. J. Cell Sci. **120:**1584–1595.
8. **Chae, H.-D., K. Lee, D. A. Williams, and Y. Gu.** 2008. Cross-talk between RhoH and Rac1 in regulation of actin cytoskeleton and chemotaxis of hematopoietic progenitor cells. Blood **111:**2597–2605.
9. **Cognetti, D., D. Davis, and J. Sturtevant.** 2002. The *Candida albicans* 14-3-3 gene, BMHI, is essential for growth. Yeast **19:**55–67.
10. **García-Pedrajas, M. D., M. Nadal, M. Bölker, S. E. Gold, and M. H. Perlin.** 2008. Sending mixed signals: redundancy versus uniqueness of signaling components in the plant pathogen, *Ustilago maydis*. Fungal Genet. Biol. **45**(Suppl. 1)**:**S22–S30.
11. **Gold, S. E., S. M. Brogdon, M. E. Mayorga, and J. W. Kronstad.** 1997. The *Ustilago maydis* regulatory subunit of a cAMP-dependent protein kinase is required for gall formation in maize. Plant Cell **9:**1585–1594.
12. **Heinrich, M., T. Köhler, and H.-U. Mösch.** 2007. Role of Cdc42-Cla4 interaction in the pheromone response of *Saccharomyces cerevisiae*. Eukaryote Cell **6:**317–327.
13. **Hlubek, A., K. Schink, M. Mahlert, B. Sandrock, and M. Bölker.** 2008. Selective activation by the guanine nucleotide exchange factor Don1 is a main determinant of Cdc42 signaling specificity in *Ustilago maydis*. Mol. Microbiol. **68:**615–623.
14. **Holliday, R.** 1974. *Ustilago maydis*, p. 575–595. *In* R. C. King (ed.), Handbook of genetics. Plenum Press, Inc., New York, NY.
15. **Hope, H., S. Bogliolo, R. A. Arkowitz, and M. Bassilana.** 2008. Activation of Rac1 by the guanine nucleotide exchange factor Dck1 is required for invasive filamentous growth in the pathogen *Candida albicans*. Mol. Biol. Cell. **19:** 3631–3651.
16. **Hurtado, C. A. R., and R. A. Rachubinski.** 2002. YlBMH1 encodes a 14-3-3 protein that promotes filamentous growth in the dimorphic yeast *Yarrowia lipolytica*. Microbiology **148:**3725–3735.
17. **Inoue, M., Y. Nakamura, K. Yasuda, N. Yasaka, T. Hara, A. Schnaufer, K. Stuart, and T. Fukuma.** 2005. The 14-3-3 proteins of *Trypanosoma brucei* function in motility, cytokinesis, and cell cycle. J. Biol. Chem. **280:**14085–14096.
18. **Irie, K., Y. Gotoh, B. M. Yashar, B. Errede, E. Nishida, and K. Matsumoto.** 1994. Stimulatory effects of yeast and mammalian 14-3-3 proteins of the Raf protein kinase. Science **265:**1716–1719.
19. **Ishiguro, J., S. Shimada, M. Gabriel, and M. Kopecká.** 2001. Characterization of a fission yeast mutant which displays in cell wall integrity and cytokinesis. Genes Genet. Syst. **76:**257–269.

20. **Kämper, J., R. Kahmann, M. Bölker, L. J. Ma, T. Brefort, B. J. Saville, F. Banuett, J. W. Kronstad, S. E. Gold, O. Müller, M. H. Perlin, H. A. Wösten, R. de Vries, J. Ruiz-Herrera, C. G. Reynaga-Peña, K. Snetselaar, M. McCann, J. Pérez-Martín, M. Feldbrügge, C. W. Basse, G. Steinberg, J. I. Ibeas, W. Holloman, P. Guzman, M. Farman, J. E. Stajich, R. Sentandreu, J. M. González-Prieto, J. C. Kennell, L. Molina, J. Schirawski, A. Mendoza-Mendoza, D. Greilinger, K. Münch, N. Rössel, M. Scherer, M. Vranes, O. Laddendorf, V. Vincon, U. Fuchs, B. Sandrock, S. Meng, E. C. Ho, M. J. Cahill, K. J. Boyce, J. Klose, S. J. Klosterman, H. J. Deelstra, L. Ortiz-Castellanos, W. Li, P. Sanchez-Alonso, P. H. Schreier, I. Häuser-Hahn, M. Vaupel, E. Koopmann, G. Friedrich, H. Voss, T. Schlüter, J. Margolis, D. Platt, C. Swimmer, A. Gnirke, F. Chen, V. Vysotskaia, G. Mannhaupt, U. Güldener, M. Münsterkötter, D. Haase, M. Oesterheld, H. W. Mewes, E. W. Mauceli, D. DeCaprio, C. M. Wade, J. Butler, S. Young, D. B. Jaffe, S. Calvo, C. Nusbaum, J. Galagan, and B. W. Birren.** 2006. Insights from the genome of the biotrophic fungal plant pathogen *Ustilago maydis*. Nature **444:**97–101.
21. **Klosterman, S. J., A. D. Martinez-Ezpinoza, D. L. Andrews, J. R. Seay, and S. E. Gold.** 2008. Ubc2, an ortholog of the yeast ste50p, possesses a basidiomycete-specific carboxy-terminal extension essential for pathogenicity independent of pheromone response. Mol. Plant-Microbe Interact. **21:**110–121.
22. **Köhli, M., S. Buck, and H.-P. Schmitz.** 2008. The function of two closely related Rho proteins is determined by an atypical switch I region. J. Cell Sci. **121:**1065–1075.
23. **Kono, K., S. Nogami, M. Abe, M. Nishizawa, S. Morishita, D. Pellman, and Y. Ohya.** 2008. G_1/S cyclin-dependent kinase regulates small GTPase Rho1p through phosphorylation of RhoGEF Tus1p in *Saccharomyces cerevisiae*. Mol. Biol. Cell **19:**1763–1771.
24. **Kronstad, J. W., and S. A. Leong.** 1989. Isolation of two alleles of the *b* locus of *Ustilago maydis*. Proc. Natl. Acad. Sci. USA **86:**978–982.
25. **Leblanc, V., B. Tocque, and I. Delumeau.** 1998. Ras-Gap controls Rho-mediated cytoskeletal reorganization through its SH3 domain. Mol. Cell. Biol. **18:**5567–5578.
26. **Leveleki, L., M. Mahlert, B. Sandrock, and M. Bölker.** 2004. The PAK family kinase Cla4 is required for budding and morphogenesis in *Ustilago maydis*. Mol. Microbiol. **54:**396–406.
27. **Lian, T., M. I. Simmer, C. A. D'Souza, B. R. Steen, S. D. Zuyderduhn, S. J. M. Jones, M. A. Marra, and J. W. Kronstad.** 2005. Iron-regulated transcription and capsule formation in the fungal pathogen *Cryptococcus neoformans*. Mol. Microbiol. **55:**1452–1472.
28. **Madaule, P., R. Axel, and A. M. Myers.** 1987. Characterization of two members of the *rho* gene family from the yeast *Saccharomyces cerevisiae*. Proc. Natl. Acad. Sci. USA **84:**779–783.
29. **Mahlert, M., K. Leveleki, A. Hlubek, B. Sandrock, and M. Bölker.** 2006. Rac1 and Cdc42 regulate hyphal growth and cytokinesis in the dimorphic fungus *Ustilago maydis*. Mol. Microbiol. **59:**567–578.
30. **Martínez-Rocha, A. L., M. I. G. Roncero, A. López-Ramirez, M. Mariné, J. Guarro, G. Martínez-Cadena, and A. Di Pietro.** 2008. Rho1 has distinct functions in morphogenesis, cell wall biosynthesis and virulence of *Fusarium oxysporium*. Cell. Microbiol. **10:**1339–1352.
31. **Mhawech, P.** 2005. 14-3-3 proteins: an update. Cell Res. **15:**228–236.
32. **Mielnichuk, N., and J. Pérez-Martín.** 2008. 14-3-3 regulates the G_2/M transition in the basidiomycete *Ustilago maydis*. Fungal Genet. Biol. **45:**1206–1215.
33. **Mishra, M., J. Karagiannis, M. Sevugan, P. Singh, and M. K. Balasubramanian.** 2005. The 14-3-3 protein Rad24p modulates function of the Cdc14p family phosphatase Clp1p/Flp1p in fission yeast. Curr. Biol. **15:**1376–1383.
34. **Müller, P., G. Weinzierl, A. Brachmann, M. Feldbrügge, and R. Kahmann.** 2003. Mating and pathogenic development of the smut fungus *Ustilago maydis* are regulated by one mitogen-activated protein kinase cascade. Eukaryot. Cell **2:**1187–1199.
35. **Nakano, K., R. Arai, and I. Mabuchi.** 1997. The small GTP-binding protein Rho1 is a multifunctional protein that regulates actin localization, cell polarity, and septum formation in the fission yeast *Schizosaccharomyces pombe*. Genes Cells **2:**679–694.
36. **Ohta, Y., J. H. Hartwig, and T. P. Stossel.** 2006. FilGAP, a Rho- and ROCK-regulated GAP for RAC binds filamin A to control actin remodeling. Nature **8:**803–814.
37. **Palmer, G. E., K. J. Johnson, S. Ghosh, and J. Sturtevant.** 2004. Mutant alleles of the essential 14-3-3 gene in *Candida albicans* distinguish between growth and filamentation. Mol. Microbiol. **150:**1911–1924.
38. **Roberts, R. L., H. U. Mosch, and G. R. Fink.** 1997. 14-3-3 proteins are essential for RAS/MAPK cascade signaling during pseudohyphal development in *Saccharomyces cerevisiae*. Cell **89:**1055–1065.
39. **Roh, D. H., B. Bowers, H. Riezman, and E. Cabib.** 2002. Rho1p mutations specific for regulation of β-1,3-glucan synthesis and the order of assembly of the yeast cell wall. Mol. Microbiol. **44:**1167–1183.
40. **Sambrook, J., and D. Russell.** 2001. Molecular cloning: a laboratory manual, 3rd ed. Cold Spring Harbor Laboratory Press, Cold Spring Harbor, NY.
41. **Sandrock, B., C. Böhmer, and M. Bölker.** 2006. Dual function of the germinal centre kinase Don3 during mitosis and cytokinesis in *Ustilago maydis*. Mol. Microbiol. **62:**655–666.
42. **Santos, B., J. Gutiérrez, T. M. Calonge, and P. Pérez.** 2003. Novel Rho GTPase involved in cytokinesis and cell wall integrity in the fission yeast *Schizosaccharomyces pombe*. Eukaryot. Cell **2:**521–533.
43. **Schulz, B., F. Banuett, M. Dahl, R. Schlesinger, W. Schäfer, and T. Martin.** 1990. The *b* alleles of *U. maydis*, whose combinations program pathogenic development, code for polypeptides containing a homeodomain-related motif. Cell **60:**295–306.
44. **Schwartz, M.** 2004. Rho signaling at a glance. Cell Science **117:**5457–5458.
45. **Schirawski, J., H. U. Böhnert, G. Steinberg, K. Snetselaar, L. Adamikowa, and R. Kahmann.** 2005. Endoplasmic reticulum glucosidase II is required for pathogenicity of *Ustilago maydis*. Plant Cell **17:**3532–3543.
46. **Smith, D. G., M. D. Garcia-Pedrajas, W. Hong, Z. Yu, S. E. Gold, and M. H. Perlin.** 2004. An *ste20* homologue in *Ustilago maydis* plays a role in mating and pathogenicity. Eukaryot. Cell **3:**180–189.
47. **Spellig, T., A. Bottin, and R. Kahmann.** 1996. Green fluorescent protein (GFP) as a new vital marker in the phytopathogenic fungus *Ustilago maydis*. Mol. Gen. Genet. **252:**503–509.
48. **Tiedje, C., I. Sakwa, U. Just, and T. Höfken.** 2008. The Rho GDI Rdi1 regulates Rho GTPases by distinct mechanisms. Mol. Biol. Cell **19:**2885–2896.
49. **Tolliday, N., L. VerPlank, and R. Li.** 2002. Rho1 directs formin-mediated actin ring assembly during budding yeast cytokinesis. Curr. Biol. **12:**1864–1870.
50. **van Hemert, M. J., Y. H. Steensma, and G. P. H. van Heusden.** 2001. 14-3-3 proteins: key regulators of cell division, signaling and apoptosis. Bioessays 2 **23:**936–946.
51. **Versele, M., and J. Thorner.** 2004. Septin collar formation in budding yeast requires GTP binding and direct phosphorylation by the PAK, Cla4. J. Cell Biol. **164:**701–715.
52. **Wadsworth, P.** Cytokinesis: Rho marks the spot. Curr. Biol. **15:**871–873.
53. **Weber, I., D. Assmann, E. Thines, and G. Steinberg.** 2006. Polar localizing class V myosin chitin synthases are essential during early plant infection in the plant pathogenic fungus *Ustilago maydis*. Plant Cell **18:**225–242.
54. **Wedlich-Soldner, R., M. Bolker, R. Kahmann, and G. Steinberg.** 2000. A putative endosomal t-SNARE links exo- and endocytosis in the phytopathogenic fungus *Ustilago maydis*. EMBO J. **19:**1974–1986.
55. **Weinzierl, G., L. Leveleki, A. Hassel, G. Kost, G. Wanner, and M. Böker.** 2002. Regulation of cell separation in the dimorphic fungus *Ustilago maydis*. Mol. Biol. **45:**219–231.
56. **Williams, M. J., M. S. Habayeb, and D. Hultmark.** 2006. Reciprocal regulation of Rac1 and Rho1 in *Drosophila* circulating immune surveillance cells. J. Cell Sci. **120:**502–521.
57. **Wójciak-Stothard, B., S. Potempa, T. Eichholtz, and A. J. Ridley.** 2001. Rho and Rac but not Cdc42 regulate endothelial cell permeability. J. Cell Sci. **114:**1343–1355.
58. **Yon, J., and M. Fried.** 1989. Precise gene fusion by PCR. Nucleic Acids Res. **17:**4895.
59. **Zanke, F. T., M. Krendel, C. DerMardirossian, C. C. King, B. P. Bohl, and G. M. Bokoch.** 2004. P21-activated kinase 1 phosphorylates and regulates 14-3-3 binding to GEF-H1, a microtubule-localized Rho exchange factor. J. Biol. Chem. **279:**18392–18400.